Journal of Pain Research

Dovepress
Taylor & Francis Group

Open Access Full Text Article

ORIGINAL RESEARCH

Resting-State Electroencephalography Networks Underlying Individual Differences in the Effects of Virtual Reality Visual Feedback on Deafferentation Pain

Shiori Kinoshita[1,2], Yu Miyawaki[2], Michihiro Osumi[1], Akihiko Murai[2]

[1]Graduate School of Health Science, Kio University, Nara, Japan; [2]Research Institute on Human and Societal Augmentation, National Institute of Advanced Industrial Science and Technology, Chiba, Japan

Correspondence: Shiori Kinoshita, Graduate School of Health Science, Kio University, 4-2-2 Umaminaka, Koryo-cho, Kitakatsuragi-gun, Nara, 635-0832, Japan, Email kinoshita.shiori.0906@gmail.com; Yu Miyawaki, Research Institute on Human and Societal Augmentation, National Institute of Advanced Industrial Science and Technology, Kashiwa II Campus, University of Tokyo, 6-2-3 Kashiwanoha, Kashiwa, Chiba, 277-0882, Japan, Tel +81-50-3522-8490, Email yu.miyawaki@aist.go.jp

Objective: Deafferentation pain refers to pain that can arise from a mismatch between motor intention and sensory feedback owing to the interruption of sensory input caused by nervous system damage. Visual feedback interventions using virtual reality (VR) have been implemented as a treatment approach to promote sensorimotor congruence. However, the degree of pain relief achieved with VR interventions varies considerably across individuals, and the neural mechanisms underlying this variability remain unclear. This study aimed to investigate the relationship between resting-state brain networks and individual differences in the effects of a VR visual feedback intervention on deafferentation pain.

Methods: We examined 10 patients with deafferentation pain. They underwent a VR intervention designed to relieve pain. Resting-state electroencephalography was recorded, and pain intensity was assessed before and after the intervention. In addition, we compared resting-state networks between the patients and 23 healthy adults.

Results: Our results demonstrated interindividual variability in pain relief that was significantly correlated with the beta band network properties, particularly small-worldness and the average clustering coefficient among nodes within the frontal region. Patients showed significantly higher small-worldness than healthy adults, along with a significantly higher average clustering coefficient across nodes within the frontal region compared with other regions. These nodes exhibited significantly stronger functional connectivity with the frontoparietal region compared with healthy adults.

Conclusion: These findings suggest that small-worldness or frontoparietal connectivity may be involved in the sensitivity to sensorimotor congruence in visual feedback interventions, thereby contributing to individual differences in pain reduction.

Keywords: virtual reality, deafferentation pain, EEG, brain network, functional connectivity

Introduction

Deafferentation pain refers to pain arising from the interruption of sensory input due to nervous system damage, such as limb amputation or brachial plexus injury. Pain occurring after limb amputation is termed phantom limb pain, characterized by painful sensations perceived in an absent limb, which is still perceived to exist. It reportedly occurs in approximately 60% of cases.[1] In addition, patients with brachial plexus injury also develop pain resembling phantom limb pain.[2] These deafferentation pains are characterized by severe spontaneous pain in body parts distal to the lesion, despite reduced or absent nociceptive responses to external stimuli,[3] leading to a decline in quality of life.[4,5] Thus, developing therapeutic strategies to alleviate deafferentation pain remains an urgent clinical challenge. A proposed mechanism underlying this pain is a mismatch between motor intention and sensory feedback.[6] Specifically, when the predicted movement generated by the efference copy

https://doi.org/10.2147/JPR.S591435
Received: 11 January 2026
Accepted: 11 May 2026
Published: 23 July 2026

does not match the actual sensory feedback, an error signal arises, which may be perceived as pain. This mechanism suggests that reducing sensorimotor incongruence helps alleviate deafferentation pain.

Visual Feedback Interventions and Individual Variability

As a therapeutic approach for deafferentation pain, interventions that manipulate visual feedback using a mirror or virtual reality (VR) system have been proposed.[7,8] These interventions aim to align internal prediction with sensory feedback by providing visual feedback of lost limb movements, thereby alleviating pain. However, previous studies have reported inconsistent effects,[9,10] suggesting that effectiveness varies across individuals. For example, one study reported that deafferentation pain severity varies according to the extent to which the phantom limb can move freely (sensorimotor consistency).[11] Conversely, an intervention that improves sensorimotor congruence through visual feedback reportedly enhances the sense of agency (SoA) over movements, without necessarily reducing pain intensity.[12] These findings suggest individual differences in sensitivity to sensorimotor congruence induced by visual feedback interventions, which may underlie the variability in pain reduction. However, the factors underlying this individual sensitivity remain unclear.

Neural Bases Associated with Deafferentation Pain

To investigate these factors, it may be useful to first analyze brain states and infer relevant factors through functional analyses. Previous studies have suggested that deafferentation pain results from plastic changes in frontoparietal regions, including the sensorimotor, anterior cingulate, and dorsolateral prefrontal cortices, because of interrupted centripetal inputs due to peripheral injury.[13–15] Among these regions, frontal areas appear particularly relevant, as an electroencephalography (EEG) study in patients with phantom limb pain demonstrated increased beta-band activity in frontal regions,[16] and such activity has been proposed to reflect changes in the descending pain modulatory system.[17] Beyond these local changes, recent evidence reported cortical reorganization at a network-level scale in the resting state, suggesting that not only local plasticity but also abnormalities in functional connectivity among multiple brain regions contribute to deafferentation pain.[18] Consistent with this view, amputees have been reported to exhibit higher small-worldness, a network metric that reflects the balance between global integration and local clustering, compared with healthy individuals.[19] This finding suggests that the overall organization of brain networks may be altered in these patients. Taken together, these findings indicate that both whole-brain network architecture and functional networks centered on frontal regions may undergo reorganization, and that the state of these networks spanning regions with diverse roles may contribute to the modulation of deafferentation pain. However, it remains unclear whether specific networks are associated with individual differences in the effects of visual feedback interventions on deafferentation pain, namely sensitivity to sensorimotor congruence.

Study Aim

This study aimed to investigate the relationship between resting-state brain networks and individual differences in the effects of a visual feedback intervention on deafferentation pain. A VR system was adopted to manipulate the visual feedback of movements in patients with deafferentation pain because VR-based interventions enable more flexible manipulations of visual feedback.[20] Resting-state EEG was chosen because recording EEG during VR interventions may introduce noise or cause electrode displacement. Using the EEG data, we performed network analyses based on graph-theoretical measures, including clustering coefficient and small-worldness, to explore individual differences in VR-induced pain relief. Among these indices, this study focused on the clustering coefficient, which constitutes a component of small-worldness, because it may reflect functional modules among brain regions (see the network indices section). This study sought to provide a better understanding of the mechanisms underlying deafferentation pain alleviation.

Materials and Methods

Participants

Ten patients with deafferentation pain (mean age = 49.8 years, SD = 14.1; two women) participated in this study. Deafferentation pain was assessed using the short-form McGill pain questionnaire 2 (SF-MPQ2), which has demonstrated high reliability and validity.[21] This scale comprises 22 items rated on an 11-point Likert scale. We conducted

a post hoc power analysis with this sample size using an effect size derived from one of our main results (Cohen's d = 0.80). This analysis indicated a statistical power of 0.62 (see Limitations).

The inclusion criteria were having deafferentation pain (SF-MPQ2 score ≥ 1) and either a history of limb amputation or a diagnosis of brachial plexus injury. The exclusion criterion was having verbal communication impairments. Clinical experts confirmed that all patients had no impairments. To confirm whether a network index associated with individual differences in VR-induced pain changes reflected abnormality, we compared resting-state networks between patients and healthy people. For this comparison, we used a sample of 23 healthy adults (mean age = 24.3 years, SD = 4.6; 11 women) obtained from another study with a different purpose. Although a between-group difference was observed in ages, we confirmed a non-significant association between the network index and age (see the Results section). A summary of the data for patients and healthy adults is presented in Supplementary Table 1. No randomization was conducted in this study. This study was approved by the Institutional Review Board (Kio University, Japan; ethics approval number R5-17) and conducted in accordance with the Declaration of Helsinki. All participants provided written informed consent before participation. This study was conducted after being registered in the UMIN Clinical Trials Registry (UMIN000051887).

VR System

Movements of the intact forearm and hands/fingers of the patients were detected and recorded using infrared motion capture systems (Kinect for Windows v2, Microsoft; Leap Motion, Leap Motion Inc). Subsequently, three-dimensional computer graphics models of their movements were generated and mirrored to create symmetrical representations. The mirror-inverted image representing a virtual limb was visually presented to patients through an immersive head-mounted display (Oculus Rift, Oculus VR) that tracked head orientation and movements to provide real-time feedback.

EEG Recording and Preprocessing

Participants were instructed to sit on a chair with their eyes closed and to remain in a resting state. EEG data were recorded from 64 channels according to the international 10–20 system using the BioSemi ActiveTwo system. Recordings were obtained under closed-eye conditions for 3 min at a sampling rate of 1,024 Hz. The recorded EEG signals were amplified across all channels and digitized. Electrode impedances were maintained below 5 kΩ throughout the recording. Pre-processing was performed using MATLAB (R2023b) and EEGLAB (v2022.1). Offline pre-processing of the EEG data included downsampling to 256 Hz and applying a 1–100 Hz band-pass filter. Given that the combination of ZapLine[22] and CleanLine[23] is reportedly effective for removing power line noise,[24] we removed the power line noise at 60 Hz using this method. Further, we performed re-referencing using the reference electrode standardization technique,[25,26] which provides a standardized reference rather than a simple average across channels. The continuous EEG was subsequently segmented into 2-s epochs with 50% overlap between consecutive epochs. Automatic epoch rejection was applied using a joint-probability criterion (single-channel 6 SD and all-channel 2 SD thresholds) to remove outlier epochs. Artifact components arising from eye blinks or muscle activity were identified using independent component analysis and were subsequently removed after a visual inspection of their characteristics.

Network Analyses

The EEG data were analyzed using the DISCOVER-EEG pipeline.[27] We used the Desikan–Killiany atlas to allocate the estimated cortical signals into 68 regions of interest (Supplementary Table 2). The frequencies of interest were alpha (8–12 Hz) and beta (13–30 Hz) bands.[19] Source-based connectivity matrices were obtained by computing amplitude envelope correlation (AEC), which was used to quantify functional connectivity as the Pearson correlation between the amplitude envelopes of the two signals. This measure has been shown to be relatively robust against the influence of volume conduction.[27] Network analysis based on graph theory was performed afterward. This analysis applied a thresholding procedure wherein the top 20% of connectivity strengths were assigned a value of 1 (edges), and all others were set to 0, yielding binary network matrices. This thresholding procedure has been reported to yield reproducible graph metrics when using AEC-based connectivity.[27] Using the binarized matrices, two local and three global network indices were calculated as follows:

Degree:

$$k_i = \sum_{j=1}^{N} A_{ij}$$

Where $A_{ij} = 1$ indicates the presence of an edge between nodes i and j, whereas $A_{ij} = 0$ indicates its absence. N represents the total number of nodes in the functional connectivity network. The degree of node i quantifies the extent to which the node is connected in the network.

Clustering coefficient:

$$C_i = \frac{2E_i}{k_i(k_i - 1)}$$

Where k_i denotes the degree of node i, and E_i represents the number of edges existing between the neighboring nodes of node i. The clustering coefficient of node i quantifies the proportion of possible triangles around the node that are actually formed, reflecting its tendency to form functional clusters with its neighbors.

Global clustering coefficient:

$$C_{\text{glob}} = \frac{1}{N} \sum_{i=1}^{N} C_i$$

Where C_i denotes the local clustering coefficient of node i, and N represents the total number of nodes in the functional connectivity network. The global clustering coefficient quantifies the overall tendency of nodes in the network to form clusters.

Global efficiency:

$$G = \frac{1}{N(N-1)} \sum_{i \neq j} \frac{1}{L_{ij}}$$

Where L_{ij} represents the shortest path length between nodes i and j, and N denotes the total number of nodes in the functional connectivity network. The global efficiency quantifies the overall efficiency of the information transfer across networks.

Small-worldness:

$$S = \frac{C_{\text{glob}}/C_{\text{rand}}}{L_{\text{glob}}/L_{\text{rand}}}$$

Where C_{glob} and C_{rand} denote the average clustering coefficients across all nodes in the observed and comparable random networks, respectively, while L_{glob} and L_{rand} represent the average shortest path lengths across all possible pairs of nodes in the observed and random networks, respectively. The small-worldness quantifies the extent to which a network exhibits small-world properties, characterized by high local clustering and short global path lengths.

Procedure

This study employed a pre–post test design. In the PRE condition, resting-state EEG was recorded, and pain intensity was evaluated using SF-MPQ2. To evaluate the SoA toward phantom or affected limb movements, we used three items selected from the questionnaire developed by Imaizumi et al,[12] each rated on a five-point Likert scale. Furthermore, we assessed the sense of ownership (SoO) toward their limbs using three other items of the same questionnaire. After the PRE condition, patients underwent a VR intervention as a rehabilitation treatment (Figure 1).[28] This intervention comprised the following tasks: (1) hand opening and closing/forearm pronation–supination tasks in a VR environment; (2) scooping up balls; and (3) collecting blocks and placing them into holes. The intervention continued for approximately 20 min. In the POST condition, pain intensity, SoA, and SoO were reassessed using questionnaires to investigate whether they improved after the intervention.

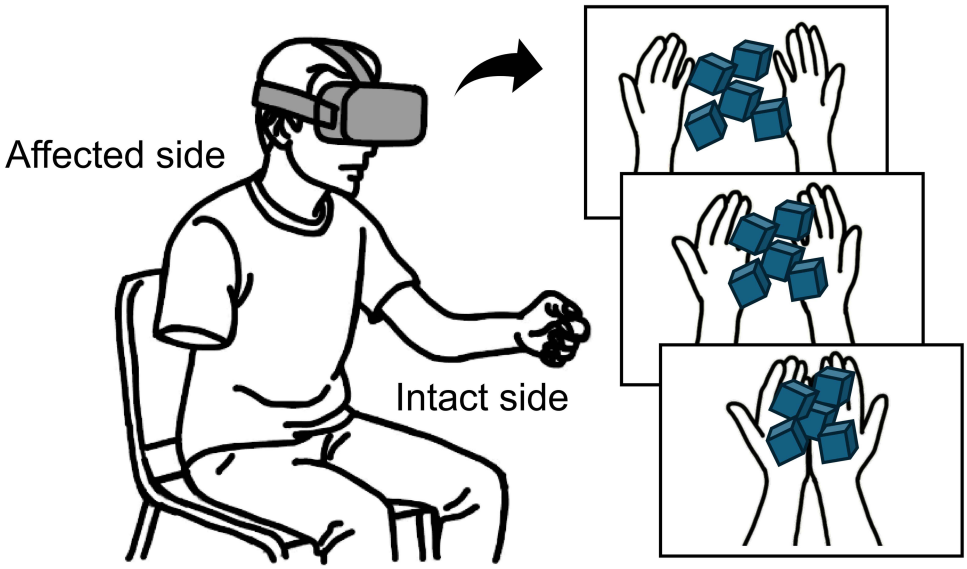

Figure 1 VR intervention. Participants wore a VR headset and performed tasks using intact and virtual limbs. The figure illustrates the action of scooping blocks in the VR environment using both the upper limbs.

Statistical Analyses

To investigate the changes in pain intensity, SoA, and SoO after the VR intervention, we first analyzed the differences between the PRE and POST conditions using paired t-tests. As additional analyses, we conducted correlation analyses of pain intensity in the PRE condition and network indices. Thereafter, we investigated the relationship between individual differences in pain relief and network indices. To quantify the individual differences, the difference in deafferentation pain between the PRE and POST conditions was calculated as an index of pain changes (DP_{dif}), with larger values indicating greater improvement. Using this variable, we performed correlation analyses with network indices. To compare the influences of a network index, SoA, and SoO on pain relief, we performed a multiple regression analysis with the network index, SoA, and SoO in the PRE condition as independent variables and DP_{dif} as a dependent variable. To investigate whether pain was alleviated through improvement in SoA or SoO, we calculated the difference in SoA (SoA_{dif}) or SoO (SoO_{dif}) between the PRE and POST conditions. We conducted mediation analyses using the network index as an independent variable, SoA_{dif} or SoO_{dif} as a mediation variable, and DP_{dif} as the dependent variable. In the multiple regression and mediation analyses, a network index that exhibited a significant correlation with the DP_{dif} was selected as an independent variable. The parameters were estimated using the maximum likelihood method.

To confirm whether the network indices identified in the above analyses reflected an abnormality, we compared the network indices between patients and healthy adults. For these comparisons, we performed Welch's t-tests for the local indices and 2×2 ANOVA with the factors of group (patient and healthy) and frequency (alpha and beta) for the global indices. Subsequently, we investigated regional differences using anatomical and functional parcellations. The anatomical regions were subdivided into the frontal, parietal, temporal, and occipital regions. Functional regions were subdivided based on the parcellations of the default, sensorimotor, executive, and frontoparietal networks.[29] For each of the four subdivided regions, the average clustering coefficient was calculated using the local clustering coefficients. For the anatomical and functional regions, we conducted one-way repeated-measures ANOVA to compare the average clustering coefficients among the four subdivided regions. To investigate whether the subdivided regions identified in these analyses were associated with changes in pain, we performed correlation analyses between the average clustering coefficient and DP_{dif}. Finally, we presented illustrations of edges and heat maps that showed the functional connectivity between nodes that constituted the subdivided region identified as significant in the above analysis and the other nodes. When comparing across regions in both the correlation and variance analyses (ie, in the correlation analyses of local network measures and in the regional analyses), multiple comparisons were corrected using the false discovery rate procedure with the Benjamini–Hochberg method. Statistical significance was set at $\alpha < 0.05$. All analyses were conducted using Mplus (version 8.10) or R software (version 4.3.0).

https://doi.org/10.2147/JPR.S591435

Results

Differences in Pain Intensity, SoA, and SoO Between the PRE and POST Conditions

Paired t-tests revealed significant differences in SoA ($t(9) = -3.47$, $p = 0.007$, Cohen's $d = -1.10$) and SF-MPQ2 ($t(9) = 2.54$, $p = 0.032$, Cohen's $d = 0.80$), but not in SoO ($t(9) = -1.88$, $p = 0.093$, Cohen's $d = -0.59$) (Figure 2). The results indicated that pain and SoA, but not SoO, were significantly improved by the VR intervention. However, the standard deviation of DP_{dif} was 49.5, indicating heterogeneity in pain changes after the intervention, with some participants showing improvement, while others did not.

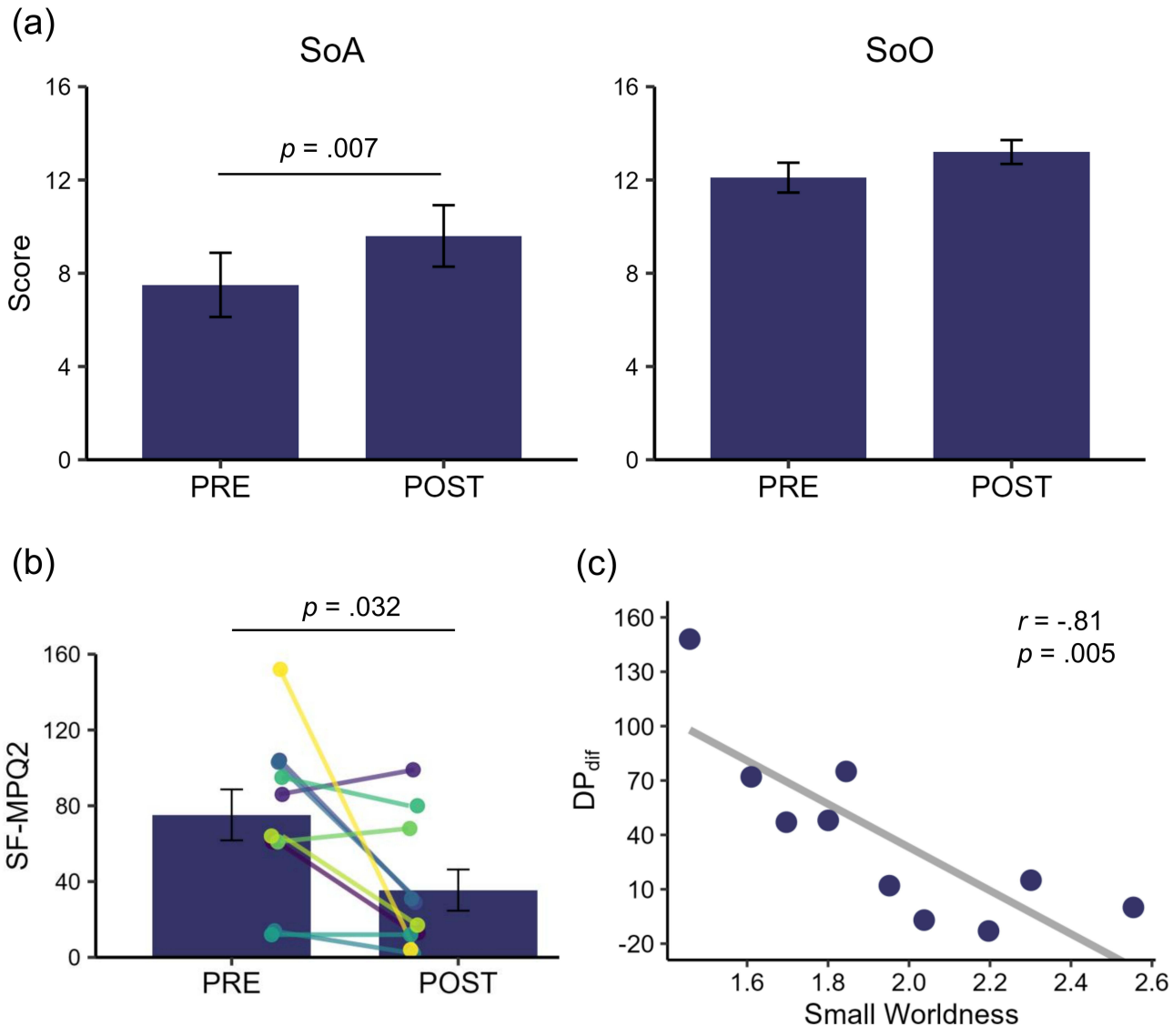

Figure 2 Changes after the VR intervention. Differences in SoA and SoO (**a**) and pain intensity (**b**) between the PRE and POST conditions. Relationship between small-worldness and pain changes (**c**). The colored lines indicate the data from individual patients, and the grey line indicates a liner regression line. DP_{dif} refers to the difference in deafferentation pain between the PRE and POST conditions.

Abbreviations: SF-MPQ2, short-form McGill pain questionnaire 2; SoA, sense of agency; SoO, sense of ownership.

Relationships Between Network Indices and Pain Changes

In the PRE condition, no significant correlations were observed between the pain intensity and any of the five network indices (Supplementary Table 3). Regarding individual differences in pain changes, a correlation analysis revealed a significant correlation between small-worldness in the beta band and DP_{dif} ($r = -0.81$, $p = 0.005$) (Figure 2); however, no significant correlations were observed with the other indices (Supplementary Table 4). These results indicate that patients exhibiting lower small-worldness in the beta band experienced greater pain relief, and vice versa.

The multiple regression analysis revealed a significant standardized path coefficient from small-worldness to DP_{dif} ($\beta = -0.77$, $p < 0.001$) but not from SoA ($\beta = 0.11$, $p = 0.55$) or SoO ($\beta = -0.17$, $p = 0.39$) to DP_{dif} (Figure 3). Further, the mediation analysis showed a significant standardized path coefficient from small-worldness to DP_{dif} after controlling for SoA_{dif} ($\beta = -0.90$, $p < 0.001$) and SoO_{dif} ($\beta = -0.79$, $p = 0.009$). Regarding the indirect effects of small-worldness on DP_{dif}, bootstrapping (resampling = 2,000) revealed bias-corrected 95% confidence intervals for SoA_{dif} (−0.05, 1.10) and SoO_{dif} (−0.75, 0.12), indicating non-significant mediation effects (detailed results are presented in Supplementary Table 5). These results indicated that pain changes after the VR intervention were not significantly associated with SoA or SoO but rather with small-worldness.

Differences in Network Indices Between Patients and Healthy Adults

Regarding the degree and clustering coefficient in the beta band, Welch's t-tests revealed significant differences between patients and healthy adults at several nodes (Supplementary Table 6). Regarding the small-worldness, in the beta band, patients showed higher small-worldness (mean = 1.95, SD = 0.32) compared with healthy adults (mean = 1.66, SD = 0.28). A 2×2 ANOVA revealed a significant interaction between the group and frequency ($F(1, 31) = 4.57$, $p = 0.041$, $\eta_p^2 = 0.13$). For the interaction, a significant simple main effect of the group was observed in the beta band ($F(1, 31) = 6.08$, $p = 0.019$, $\eta_p^2 = 0.16$), but not in the alpha band ($F(1, 31) = 0.02$, $p = 0.89$, $\eta_p^2 < 0.001$) (Figure 4). Conversely, no significant group effects were observed in the global clustering coefficient ($ps \geq 0.058$) or global efficiency ($ps \geq 0.57$). To confirm the effect of age, we conducted a correlation analysis with the small-worldness. The result indicated no significant correlation coefficient between the small-worldness and age in patients ($r = 0.12$, $p = 0.74$) or healthy adults ($r = 0.04$, $p = 0.86$). These results indicated that patients exhibited significantly higher small-worldness in the beta band than that in healthy adults.

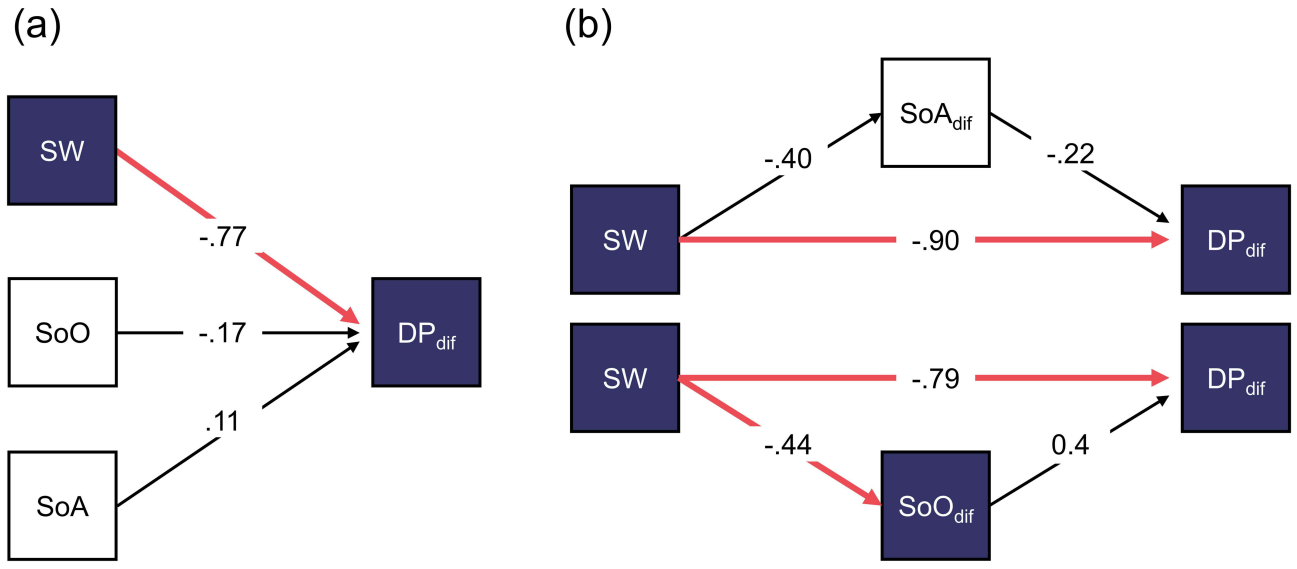

Figure 3 Influence of the small-worldness on pain changes after the VR intervention. A multiple regression (**a**) and mediation (**b**) analysis. The red arrows indicate paths that were significant in the multiple regression or mediation analyses. DP_{dif} refers to a difference in deafferentation pain between the PRE and POST conditions. SoA_{dif} and SoO_{dif} refer to differences in the senses of agency and ownership between the PRE and POST conditions, respectively.
Abbreviation: SW, small-worldness.

https://doi.org/10.2147/JPR.S591435

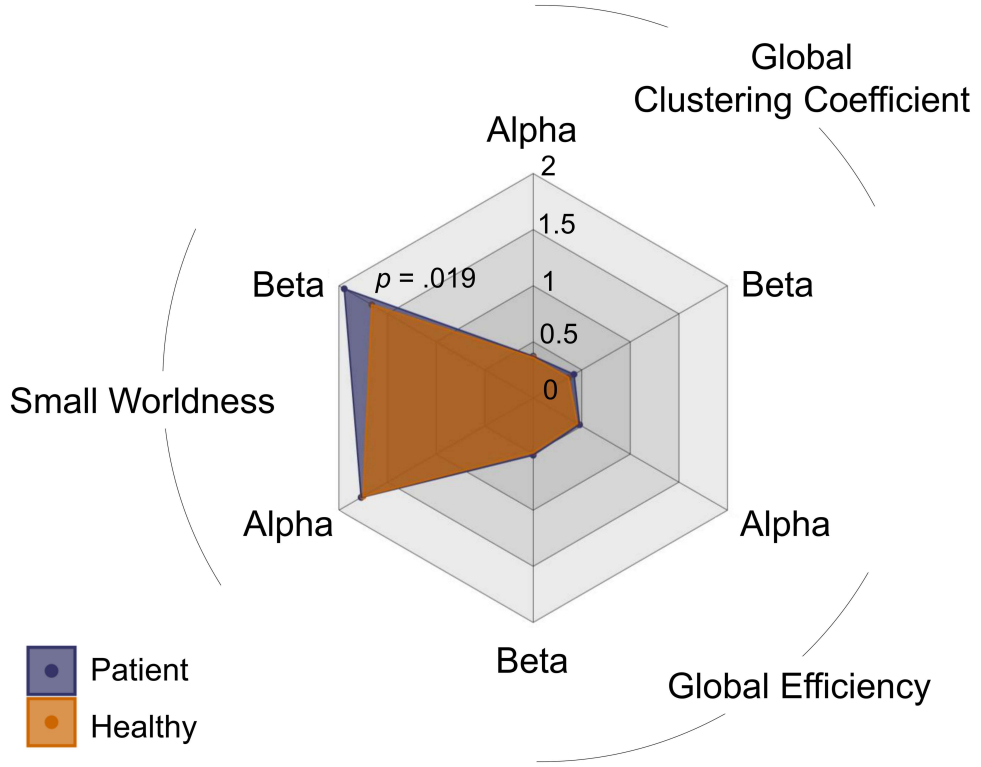

Figure 4 Differences in global indices between patients and healthy adults.

As significant differences were observed between patients and healthy adults in the beta band, we calculated its average clustering coefficient. For anatomical and functional regions, neither the patients nor the healthy adults showed significant left–right differences (adj. *p*s ≥ 0.11). In the anatomical regions, one-way repeated-measures ANOVA showed significant differences in patients ($F(3, 27) = 5.76$, $p = 0.004$, $\eta_p^2 = 0.39$) and healthy adults ($F(3, 66) = 3.15$, $p = 0.031$, $\eta_p^2 = 0.13$). Post-hoc analyses revealed that the frontal region was significantly higher than the parietal region ($t(9) = 4.31$, adj. $p = 0.012$, Cohen's $d = 1.36$) or the temporal region ($t(9) = 3.85$, adj. $p = 0.012$, Cohen's $d = 1.22$) (Figure 5). Conversely, no significant differences among the regions were observed in healthy adults (adj. *p*s ≥ 0.13). Regarding the functional regions, one-way repeated-measures ANOVA indicated a significant difference in patients ($F(3, 27) = 3.52$, $p = 0.028$, $\eta_p^2 = 0.28$), but not in healthy adults ($F(3, 66) = 1.63$, $p = 0.19$, $\eta_p^2 = 0.07$). Post-hoc analyses for patients revealed that the executive network was significantly higher than the default ($t(9) = 3.79$, adj. $p = 0.026$, Cohen's $d = 1.20$) or frontoparietal network ($t(9) = 3.20$, adj. $p = 0.032$, Cohen's $d = 1.01$), whereas those for healthy adults showed non-significant differences (adj. *p*s ≥ 0.19). These results indicated that in patients, the average clustering coefficient in the frontal region or executive network was significantly higher than that in other regions. Regarding the relationships between their average clustering coefficients and DP_{dif}, correlation analyses revealed significant correlations with the frontal region ($r = -0.71$, $p = 0.021$) and executive network ($r = -0.87$, $p = 0.001$).

To confirm which nodes were associated with the frontal region or executive network, we illustrated edges present in ≥30% of patients or healthy adults (Figure 6). The images indicated that many patients exhibited edges between the identified nodes and the frontoparietal area, whereas such connections were absent in healthy adults. Furthermore, heat maps were generated to illustrate the functional connectivity between these nodes and all 68 nodes (Figure 6). In patients, these nodes showed weak functional connectivity with nodes in the temporal and occipital areas, a pattern similar to that observed in healthy adults. However, patients exhibited stronger functional connectivity than healthy adults between these nodes and those in the frontoparietal area. Accordingly, we computed the mean functional connectivity across all connections between these nodes and the frontoparietal area across both hemispheres, and compared this value between patients and healthy adults. Welch's t-tests revealed significant differences between patients and healthy adults in the

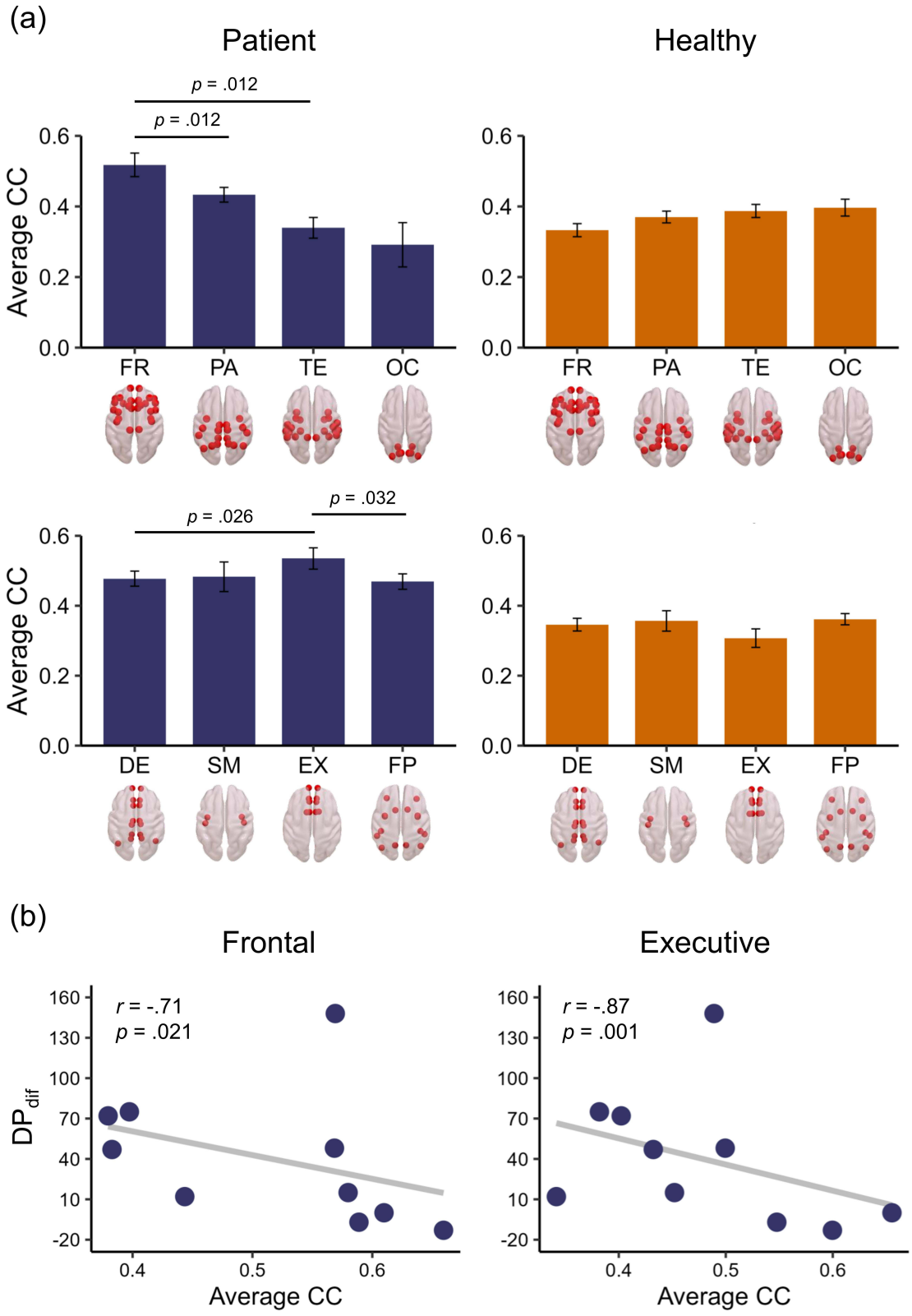

Figure 5 Average clustering coefficients. Average clustering coefficients of four anatomical and functional regions in patients and healthy adults (**a**). Relationship between pain changes and an average clustering coefficient of the frontal region or executive network (**b**). Red dots in the brain images indicate nodes that constitute each anatomical or functional region. DP_{dif} refers to the difference in deafferentation pain between the PRE and POST conditions.

Abbreviations: Average CC, average clustering coefficient; DE, default mode network; EX, executive network; FP, frontoparietal network; FR, frontal region; OC, occipital region; PR, parietal region; SM, sensorimotor network; TE, temporal region.

https://doi.org/10.2147/JPR.S591435

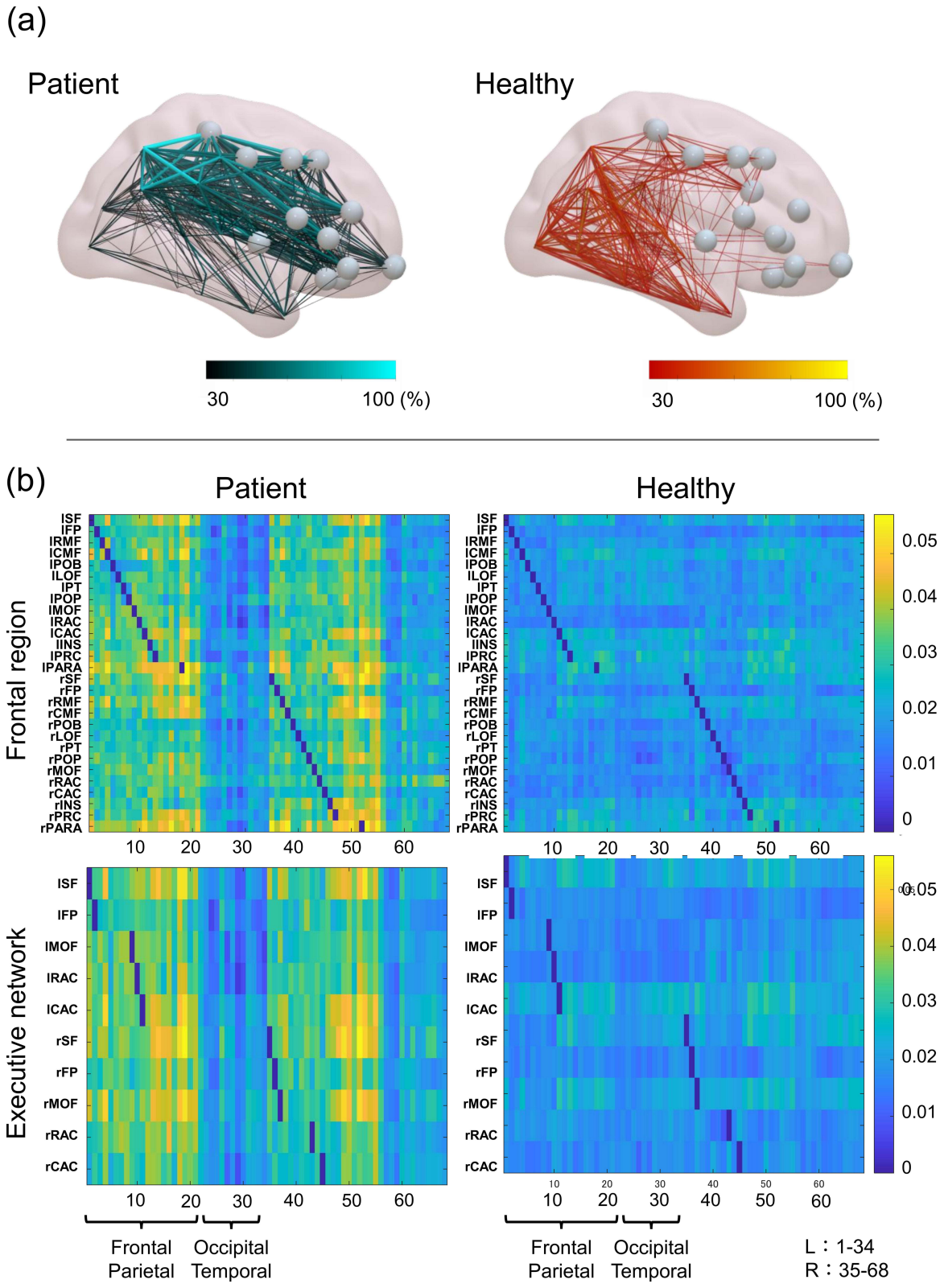

Figure 6 Networks in two groups. Edges present in ≥30% of patients or healthy adults (**a**). Connectivity matrices of nodes constituting the frontal or executive network in patients and healthy adults (**b**). Grey points represent nodes constituting the frontal region or executive network. Node names are listed in Supplementary Table 2.

https://doi.org/10.2147/JPR.S591435

anatomical region: $t(12.09) = 3.40$, $p = 0.005$, Cohen's $d = 1.55$, and the functional region: $t(12.55) = 3.41$, $p = 0.005$, Cohen's $d = 1.52$. The results indicated that the frontoparietal functional connectivity in patients was significantly stronger than that in healthy adults.

Discussion

This study aimed to investigate the relationship between resting-state brain networks and individual differences in the effects of a VR visual feedback intervention on deafferentation pain. Our results demonstrated that VR intervention significantly reduced pain intensity, supporting the effects of the VR intervention on deafferentation pain.[20] Moreover, SoA was significantly enhanced by VR intervention, whereas SoO remained unchanged. This dissociation between SoA and SoO is consistent with previous research proposing that the two are conceptually distinct[30] and are generated through different mechanisms.[31] SoO is primarily based on afferent multisensory integration, including tactile and proprioceptive signals.[32] Conversely, SoA is shaped by the congruence between motor prediction and sensory feedback.[33,34] Based on these findings, it is plausible that visual feedback interventions preferentially facilitated SoA over SoO.

Despite improvements in pain intensity and SoA, no significant correlation was observed between them. This finding reflects the ongoing debate in the literature regarding the relationship between agency and pain experience. For instance, one study reported that participants who experienced strong SoA over a virtual limb during VR-mirror therapy reported pain reduction.[35] Conversely, another study found no significant association between SoA and pain relief.[12] The lack of a consistent relationship between SoA and deafferentation pain in previous studies is reflected in our findings, further supporting the view that improvements in SoA do not necessarily mediate pain reduction. These findings suggest that VR-induced pain relief does not depend on the experience of agency itself, but rather on sensorimotor congruence. Furthermore, we observed substantial inter-individual variability in pain changes following the VR intervention; although some participants experienced notable improvements, others showed minimal or no change, highlighting the necessity of identifying the factors that may modulate sensitivity to sensorimotor congruence. Thus, we focused on resting-state EEG network features and investigated whether baseline brain organization could predict pain outcomes.

Among the network indices, small-worldness in the beta band was negatively correlated with improvement in deafferentation pain; individuals exhibiting higher beta-band small-worldness experienced less pain relief, and vice versa. Mathematically, higher small-worldness indicates greater clustering between nodes (triangles) throughout the brain. However, this may not necessarily indicate a more normal or optimal brain state, particularly in clinical settings. Amputees exhibit higher small-worldness in the alpha band than do healthy controls,[19] suggesting that such increases may reflect pathological reorganization rather than efficient processing. Our results, although involving the beta band, indicated that small-worldness was significantly higher in patients than in healthy adults, aligning with this interpretation. These findings suggest that elevated small-worldness reflects abnormal connectivity patterns that can hinder therapeutic effects.

To further explore regional network contributions, we investigated clustering coefficients at anatomical and functional levels. Although the global clustering coefficient was not significantly associated with changes in pain, regional analyses revealed that in patients, but not in healthy adults, nodes within the frontal region or executive network exhibited a higher average clustering coefficient than those in other regions. These beta-band coefficients were negatively correlated with pain improvement. An EEG study on patients with phantom limb pain reported increased frontal beta activity,[16] which has been widely reported in other pain syndromes.[36,37] Such activity may reflect alterations in descending pain modulation pathways.[17] In this study, non-significant correlations were observed between network indices and pain intensity in the PRE condition. Considering these findings, our results suggest that individuals with elevated frontal beta connectivity have impaired descending pain control, rendering them less responsive to sensorimotor congruence through a visual feedback intervention.

Nodes within the frontal region or executive network exhibited enhanced connectivity with frontoparietal nodes in patients. The frontal cortex plays a crucial role in cognitive pain appraisal.[17] Meanwhile, the parietal cortex is implicated in the sensory-discriminative aspects of pain. Reorganization of the primary somatosensory cortex located in the parietal region is associated with severity in phantom limb pain.[14,38] Thus, the excessive connectivity between these regions might reflect the unmasking or strengthening of previously silent or subthreshold connections.[13,19] Such abnormal connectivity patterns have been observed at local[39] and network levels,[18] suggesting that they are functionally relevant

to deafferentation pain. Overall, this study suggested that the frontoparietal system, which is involved in pain modulation or characterization, can modulate sensitivity to sensorimotor congruence in visual feedback interventions, thereby contributing to individual differences in pain reduction. These findings highlight the need for further research to investigate the relationship between the frontoparietal system and VR-induced pain changes.

Limitations

This study had some limitations. First, healthy adults could not be matched to patients in terms of age and sample size because healthy adult data were originally collected for a different research purpose. Although we confirmed that no significant correlations existed between age and the network index in either group, examining correlations with age alone does not sufficiently control for other factors that may differ between the two samples. In addition, differences in data collection conditions may compromise the validity of comparisons between the patient and healthy groups. Therefore, the comparative findings between patients and healthy adults should be interpreted with caution, and conducting the study under matched conditions would have been preferable to minimize potential confounding effects.

Second, the sample size was limited to only 10 participants because recruiting patients with deafferentation pain was challenging. This small sample size reduced statistical power, raising concerns about the potential inflation of both Type I and Type II error risks. Future studies with larger samples will be necessary to confirm these results. Third, EEG recordings were not obtained during or after the VR intervention. Only resting-state EEG data before the intervention were analyzed primarily because of concerns about noise during the intervention and participant burden. Future studies should collect EEG data before, after, and potentially during VR interventions to enable the analysis of brain network changes associated with VR effects. Such analyses may help identify longitudinal or causal relationships between brain networks and the effects of VR interventions.

Finally, this study did not include a control group for the VR intervention. Therefore, it is not possible to determine whether the observed pain relief was attributable to specific VR effects or to non-specific factors, such as the passage of time or expectancy effects. Nevertheless, the primary aim of this study was not to evaluate the efficacy of the VR intervention, but rather to analyze the relationship between VR-induced effects and network indices. Network indices detected in the analyses were elevated compared with those in healthy adults, suggesting that they reflect aberrant network properties. Thus, it is possible that these indices are associated with pain modulation in response to the VR intervention. Furthermore, pain and SoA significantly improved after the intervention, whereas SoO did not. These results are consistent with predictions based on the underlying mechanisms of these constructs. Overall, our findings appear to reflect the influence of sensorimotor congruency rather than mere time effects or expectancy bias. To further validate this possibility, future intervention studies incorporating appropriate control groups are warranted. Considering these limitations, this study should be regarded as preliminary, and future investigations will be necessary to address these constraints.

Conclusions

This study demonstrated that, although the VR visual feedback intervention alleviated deafferentation pain, the degree of pain relief varied substantially across individuals. This variability was significantly associated with small-worldness in the beta band, which was significantly higher than that in healthy adults. Notably, patients had significantly higher average clustering coefficients across nodes within the frontal region than those in other regions, whereas healthy adults did not. These nodes exhibited enhanced connectivity with the frontoparietal region, which may reflect an altered system involved in pain modulation or characterization. These preliminary findings suggest that small-worldness or frontoparietal connectivity is involved in sensitivity to sensorimotor congruence in visual feedback interventions. Therefore, these network properties might contribute to individual differences in pain reduction. However, considering the small sample size and the absence of age-matched controls, these results should be interpreted with caution. Further studies are needed to validate and extend these findings.

Abbreviations

EEG, electroencephalography; AEC, amplitude envelope correlation; SoA, sense of agency; SoO, sense of ownership; SF-MPQ2, short-form McGill pain questionnaire 2; VR, virtual reality.

Data Sharing Statement

Detailed data is available upon reasonable request from the corresponding author, SK.

Acknowledgments

We thank Yuki Morikawa, a graduate student at Kio University, for his assistance with the EEG measurements.

Author Contributions

All authors made a significant contribution to the work reported, whether that is in the conception, study design, execution, acquisition of data, analysis and interpretation, or in all these areas; took part in drafting, revising or critically reviewing the article; gave final approval of the version to be published; have agreed on the journal to which the article has been submitted; and agree to be accountable for all aspects of the work.

Funding

This study was supported by the Japan Society for the Promotion of Science (JSPS) KAKENHI [grant number 23K10442].

Disclosure

The authors declare that they have no conflicts of interest in this work.

References

1. Diers M, Krumm B, Fuchs X, et al. The prevalence and characteristics of phantom limb pain and non-painful phantom phenomena in a nationwide survey of 3,374 unilateral limb amputees. *J Pain*. 2022;23(3):411–423. doi:10.1016/j.jpain.2021.09.003
2. Shankar H, Hansen J, Thomas K. Phantom pain in a patient with brachial plexus avulsion injury. *Pain Med*. 2015;16(4):777–781. doi:10.1111/pme.12635
3. Hanakawa T. Neural mechanisms underlying deafferentation pain: a hypothesis from a neuroimaging perspective. *J Orthop Sci*. 2012;17(3):331–335. doi:10.1007/s00776-012-0209-9
4. Kuffler DP. Coping with phantom limb pain. *Mol Neurobiol*. 2018;55(1):70–84. doi:10.1007/s12035-017-0718-9
5. Ciaramitaro P, Padua L, Devigili G, et al. Prevalence of neuropathic pain in patients with traumatic brachial plexus injury: a multicenter prospective hospital-based study. *Pain Med*. 2017;18(12):2428–2432. doi:10.1093/pm/pnw360
6. Harris AJ. Cortical origin of pathological pain. *Lancet*. 1999;354(9188):1464–1466. doi:10.1016/S0140-6736(99)05003-5
7. Ramachandran VS, Rogers-Ramachandran D. Synaesthesia in phantom limbs induced with mirrors. *Proc Biol Sci*. 1996;263(1369):377–386 doi:10.1098/rspb.1996.0058.
8. Perry BN, Mercier C, Pettifer SR, Cole J, Tsao JW. Virtual reality therapies for phantom limb pain. *Eur J Pain*. 2014;18(7):897–899. doi:10.1002/ejp.559
9. Herrador Colmenero L, Perez Marmol JM, Martí-García C, et al. Effectiveness of mirror therapy, motor imagery, and virtual feedback on phantom limb pain following amputation: a systematic review. *Prosthet Orthot Int*. 2018;42(3):288–298. doi:10.1177/0309364617740230
10. Dunn J, Yeo E, Moghaddampour P, Chau B, Humbert S. Virtual and augmented reality in the treatment of phantom limb pain: a literature review. *NeuroRehabilitation*. 2017;40(4):595–601. doi:10.3233/NRE-171447
11. Sumitani M, Miyauchi S, McCabe CS, et al. Mirror visual feedback alleviates deafferentation pain, depending on qualitative aspects of the pain: a preliminary report. *Rheumatol Oxf Engl*. 2008;47(7):1038–1043. doi:10.1093/rheumatology/ken170
12. Imaizumi S, Asai T, Koyama S. Agency over phantom limb enhanced by short-term mirror therapy. *Front Hum Neurosci*. 2017;11:483. doi:10.3389/fnhum.2017.00483
13. Flor H, Nikolajsen L, Staehelin Jensen T. Phantom limb pain: a case of maladaptive CNS plasticity? *Nat Rev Neurosci*. 2006;7(11):873–881. doi:10.1038/nrn1991
14. Karl A, Birbaumer N, Lutzenberger W, Cohen LG, Flor H. Reorganization of motor and somatosensory cortex in upper extremity amputees with phantom limb pain. *J Neurosci*. 2001;21(10):3609–3618. doi:10.1523/JNEUROSCI.21-10-03609.2001
15. Preissler S, Feiler J, Dietrich C, Hofmann GO, Miltner WHR, Weiss T. Gray matter changes following limb amputation with high and low intensities of phantom limb pain. *Cereb Cortex*. 2013;23(5):1038–1048. doi:10.1093/cercor/bhs063
16. Kleeva D, Soghoyan G, Biktimirov A, et al. Modulations in high-density EEG during the suppression of phantom-limb pain with neurostimulation in upper limb amputees. *Cereb Cortex*. 2024;34(2):bhad504. doi:10.1093/cercor/bhad504
17. Bräscher AK, Becker S, Hoeppli ME, Schweinhardt P. Different brain circuitries mediating controllable and uncontrollable pain. *J Neurosci*. 2016;36(18):5013–5025. doi:10.1523/JNEUROSCI.1954-15.2016

18. Makin TR, Filippini N, Duff EP, Henderson Slater D, Tracey I, Johansen-Berg H. Network-level reorganisation of functional connectivity following arm amputation. *NeuroImage*. 2015;114:217–225. doi:10.1016/j.neuroimage.2015.02.067
19. Lyu Y, Guo X, Wang Z. Resting-state EEG network change in alpha and beta bands after upper limb amputation. 2016 38th Annual International Conference of the IEEE Engineering in Medicine and Biology Society (EMBC); IEEE; 2016:49–52. doi:10.1109/EMBC.2016.7590637
20. Gan D, Wang SY, Liu K, et al. Innovative exploration of phantom limb pain treatment based on extended reality technology. *World J Orthop*. 2025;16(6):107422. doi:10.5312/wjo.v16.i6.107422
21. Dworkin RH, Turk DC, Revicki DA, et al. Development and initial validation of an expanded and revised version of the short-form Mcgill pain questionnaire (SF-MPQ-2). *Pain*. 2009;144(1–2):35–42. doi:10.1016/j.pain.2009.02.007
22. de Cheveigné A, de Cheveigné A. ZapLine: a simple and effective method to remove power line artifacts. *NeuroImage*. 2020;207:116356. doi:10.1016/j.neuroimage.2019.116356
23. Bigdely-Shamlo N, Mullen T, Kothe C, Su KM, Robbins KA. The PREP pipeline: standardized preprocessing for large-scale EEG analysis. *Front Neuroinf*. 2015;9:16. doi:10.3389/fninf.2015.00016
24. Miyakoshi M, Schmitt LM, Erickson CA, Sweeney JA, Pedapati EV. Can we push the "quasi-perfect artifact rejection" even closer to perfection? *Front Neuroinf*. 2020;14:597079. doi:10.3389/fninf.2020.597079
25. Dong L, Li F, Liu Q, et al. MATLAB toolboxes for reference electrode standardization technique (REST) of scalp EEG. *Front Neurosci*. 2017;11:601. doi:10.3389/fnins.2017.00601
26. Dong L, Liu X, Zhao L, et al. A comparative study of different EEG reference choices for event-related potentials extracted by independent component analysis. *Front Neurosci*. 2019;13:1068. doi:10.3389/fnins.2019.01068
27. Ávila C G, Bott FS, Tiemann L, et al. DISCOVER-EEG: an open, fully automated EEG pipeline for biomarker discovery in clinical neuroscience. *Sci Data*. 2023;10(1):613. doi:10.1038/s41597-023-02525-0
28. Osumi M, Inomata K, Inoue Y, Otake Y, Morioka S, Sumitani M. Characteristics of phantom limb pain alleviated with virtual reality rehabilitation. *Pain Med*. 2019;20(5):1038–1046. doi:10.1093/pm/pny269
29. Smith SM, Fox PT, Miller KL, et al. Correspondence of the brain's functional architecture during activation and rest. *Proc Natl Acad Sci U S A*. 2009;106(31):13040–13045. doi:10.1073/pnas.0905267106
30. Gallagher I. Philosophical conceptions of the self: implications for cognitive science. *Trends Cognit Sci*. 2000;4(1):14–21. doi:10.1016/S1364-6613(99)01417-5
31. Braun N, Debener S, Spychala N, et al. The senses of agency and ownership: a review. *Front Psychol*. 2018;9(9):535. doi:10.3389/fpsyg.2018.00535
32. Tsakiris M, Longo MR, Haggard P. Having a body versus moving your body: neural signatures of agency and body-ownership. *Neuropsychologia*. 2010;48(9):2740–2749. doi:10.1016/j.neuropsychologia.2010.05.021
33. Blakemore SJ, Wolpert DM, Frith CD. Abnormalities in the awareness of action. *Trends Cognit Sci*. 2002;6(6):237–242. doi:10.1016/S1364-6613(02)01907-1
34. Frith CD, Blakemore SJ, Wolpert DM. Abnormalities in the awareness and control of action. *Philos Trans R Soc Lond B Biol Sci*. 2000;355(1404):1771–1788. doi:10.1098/rstb.2000.0734
35. Cole J, Crowle S, Austwick G, Slater DH. Exploratory findings with virtual reality for phantom limb pain; from stump motion to agency and analgesia. *Disabil Rehabil*. 2009;31(10):846–854. doi:10.1080/09638280802355197
36. Vanneste S, Ost J, Van Havenbergh T, De Ridder D. Resting state electrical brain activity and connectivity in fibromyalgia. *PLoS One*. 2017;12(6):e0178516. doi:10.1371/journal.pone.0178516
37. Stern J, Jeanmonod D, Sarnthein J. Persistent EEG overactivation in the cortical pain matrix of neurogenic pain patients. *NeuroImage*. 2006;31(2):721–731. doi:10.1016/j.neuroimage.2005.12.042
38. Flor H, Elbert T, Knecht S, et al. Phantom-limb pain as a perceptual correlate of cortical reorganization following arm amputation. *Nature*. 1995;375(6531):482–484. doi:10.1038/375482a0
39. Andoh J, Milde C, Diers M, et al. Assessment of cortical reorganization and preserved function in phantom limb pain: a methodological perspective. *Sci Rep*. 2020;10(1):11504. doi:10.1038/s41598-020-68206-9